Single-molecule magnets: isomeric $[Mn_{12}O_{12}(O_2CC_6H_4Me\text{-}4)_{16}(H_2O)_4]$ complexes exhibiting different rates of resonant magnetization tunnelling

Sheila M. J. Aubin,[a] Ziming Sun,[a] Ilia A. Guzei,[b] Arnold L. Rheingold,*[b] George Christou*[c] and David N. Hendrickson*[a]

[a] *Department of Chemistry and Biochemistry-0358, University of California at San Diego, La Jolla, CA 92093-0358, USA*
[b] *Department of Chemistry and Biochemistry, University of Delaware, Newark, DE 19716, USA*
[c] *Department of Chemistry, Indiana University, Bloomington, IN 47405-4001, USA*

Two different isomeric forms of $[Mn_{12}O_{12}(O_2CC_6H_4Me\text{-}4)_{16}(H_2O)_4]$, differing in the positioning of H_2O ligands, are structurally characterized and shown to have considerably different magnetization hysteresis loops.

Single-molecule magnets have attracted considerable attention.[1–3] The presence of appreciable magnetic anisotropy in a big spin ground-state molecule leads to a potential-energy barrier for reversal of the direction of magnetization and an isolated molecule exhibits hysteresis in its magnetization *vs.* magnetic field response. The most thoroughly studied[4,5] single-molecule magnet $[Mn_{12}O_{12}(O_2CMe)_{16}(H_2O)_4]$ **1** has a magnetization that decays with a half-life of 2 months at 2.0 K after a magnetic field is removed. One of the most interesting aspects of complex **1** is that there are steps observed at regular intervals of magnetic field in the magnetization loop for oriented crystals. These steps have been attributed[6–8] to resonant magnetization tunnelling. We herein describe the preparation and X-ray structures of two new single-molecule magnets, $[Mn_{12}O_{12}(O_2CC_6H_4Me\text{-}4)_{16}(H_2O)_4]\cdot 3H_2O$ **2** and $[Mn_{12}O_{12}(O_2CC_6H_4Me\text{-}4)_{16}(H_2O)_4]\cdot HO_2CC_6H_4Me\text{-}4$ **3**, that differ in their space group and the positioning of their H_2O ligands on the Mn_{12} complexes.

The reaction of $Mn(ClO_4)_2$ (11 mmol) with $NBu^n{}_4[MnO_4]$ (4.3 mmol) and 4-methylbenzoic acid (140 mmol) in ethanol gives complexes **2** and **3**. When anhydrous ethanol is used complex **3** results, whereas a 20% H_2O–80% EtOH reaction medium yields the hydrate complex **2**. X-Ray quality crystals of **2** and **3** were grown from a CH_2Cl_2–hexanes mixture.

The structure† of complex **2** shows a Mn_{12} complex with a $[Mn_{12}(\mu_3\text{-}O)_{12}]$ core, comprising a central $[Mn^{IV}{}_4O_4]^{8+}$ cubane held within a non-planar ring of eight Mn^{III} ions by eight μ_3-O^{2-} ions. Peripheral ligation of complex **2** is provided by sixteen η^2,μ-carboxylate groups and four H_2O ligands. The eight Mn^{III} ions fall into two groups of four Mn^{III} ions. In group I each Mn^{III} ion is bonded to a single Mn^{IV} *via* two μ_3-O^{2-} bridges, while in group II each Mn^{III} is bonded to two Mn^{IV} ions *via* two μ_3-O^{2-} bridges. The four H_2O ligands coordinate only to Mn^{III} ions in group II. Complex **2** has two H_2O ligands bonded to one Mn^{III} ion and one H_2O ligand on each of two other Mn^{III} ions. The structure† of complex **3** shows that it is an isomer of the same Mn_{12} complex. A drawing showing a superposition of the two Mn_{12} complexes is shown in Fig. 1. It can be seen that the Mn_{12} complexes in complexes **2** and **3** differ in the positioning of the four H_2O ligands. Consequential rearrangements in the 4-methybenzoate ligands also occur.

Out-of-phase ac magnetic susceptibility (χ_M'') signals are seen for both complexes **2** and **3**. Fig. 2 shows a plot for χ_M'' *vs.* T for complex **3** (upper) and for hydrated complex **2** (lower) in the region 2–10 K, measured at frequencies of 50, 250 or 1000 Hz. Both samples of these two complexes exhibit two frequency-dependent χ_M'' ac peaks, one in the region 2–4 K and the other in the region 4–7 K. However, complex **3** has predominantly a peak in the region 2–4 K, whereas hydrated complex **2** has predominantly a peak in the region 4–7 K. Several crystalline samples of $[Mn_{12}O_{12}(O_2CC_6H_4Me\text{-}4)_{16}(H_2O)_4\cdot xH_2O\cdot yHO_2CC_6H_4Me\text{-}4$ were prepared by varying the level of dryness of the EtOH reaction medium. As x and y varied, so did the intensity ratio of the two χ_M'' peaks.

Fig. 3 shows magnetization hysteresis data obtained for oriented crystal samples of complexes **2** and **3**. A few small crystals of a given complex were suspended in eicosane at 40 °C, oriented in a 5.5 kG field and then the eicosane matrix was cooled to room temp. This gives a waxy cube with the crystals aligned with their easy axes of magnetization parallel. Steps are seen in the hysteresis loops for both complexes. The sample of complex **2** is first magnetically saturated in a +3.5 kG field. All of the complexes at 2.0 K will be in the $m_s = -10$ level of the $S = 10$ double-well potential. When the field is decreased to zero, each of the $m_s = -10, -9, -8, \cdots -1, 0$ levels on the right-hand side of the double well become equal in energy to the corresponding $m_s = 10, 9, 8, \cdots 1, 0$ level of the left-hand side. As the field is decreased from +3.5 kG to zero, there is the first step at zero field. The energy alignment leads to a resonant magnetization tunnelling. Individual molecules tunnel from one $m_s < 0$ level to an $m_s > 0$ level. If all molecules

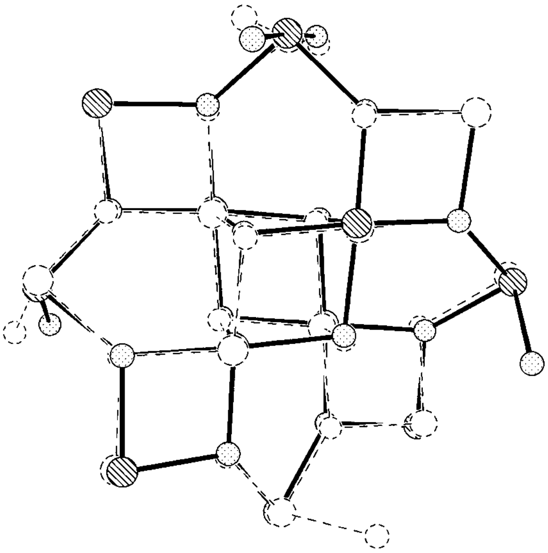

Fig. 1 Drawing showing a superposition of the cores, without 4-methylbenzoate ligands, of the $[Mn_{12}O_{12}(O_2CC_6H_4Me\text{-}4)_{16}(H_2O)_4]$ molecules in complexes **2** (---) and **3** (—). The crosshatched and stippled spheres represent manganese and oxygen atoms, respectively, in the structure of **3**. The two isomers differ in the arrangements of four H_2O ligands. Complex **2** has a 1,1,2 pattern of H_2O ligand positions, where one H_2O ligand is bonded to the Mn atom at the bottom of the drawing, one to the Mn atom at the left and two H_2O ligands bonded to the 'top' Mn atom. Complex **3** has a 1,2,1 pattern of H_2O ligands.

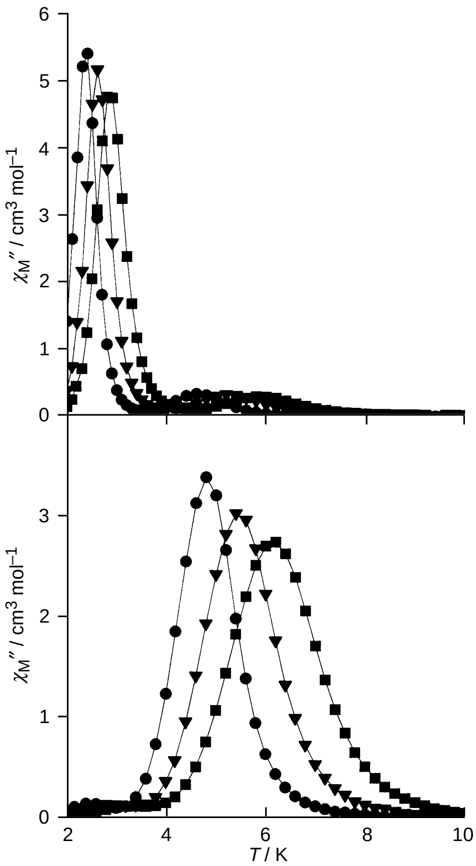

Fig. 2 Plots of the out-of-phase ac magnetic susceptibility χ_M'' *vs.* temperature for polycrystalline samples of the Mn_{12} complexes **2** (lower) and **3** (upper). Data were collected with zero dc magnetic field and with an 1.0 G ac field oscillating at: (●) 50; (▼) 250 and (■) 1000 Hz.

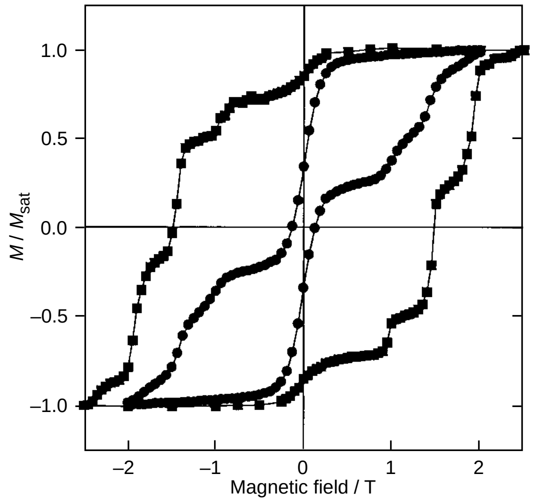

Fig. 3 Magnetization hysteresis loops measured at 1.90 K for oriented crystals in eicosane matrix for complexes **2** (■) and **3** (●). The magnetization for each complex is plotted in units of the saturation magnetization M_{sat} for that complex. The saturation magnetization values for complexes **2** and **3** are 1.20×10^5 and 1.05×10^5 cm^3 G mol^{-1}, respectively.

changed their direction of magnetization by thermal activation over the barrier, then the hysteresis loop would be a smooth function with no steps.

As can be seen in Fig. 3, it is of considerable interest to note there are appreciable differences in step heights between complexes **2** and **3**. The hysteresis loop of hydrated complex **2** is similar to that reported[6–8] for the acetate complex **1**. On the other hand, complex **3** shows a much steeper step at zero field than does complex **2**. Thus, complex **3** is exhibiting an appreciably faster rate of tunnelling of the magnetization than does complex **2**. This is the case in spite of the fact that complexes **2** and **3** have the same ligands and differ in their arrangements of four H_2O ligands and space groups. The greater rate of tunnelling for complex **3** is consistent with the fact that this complex shows its χ_M'' ac signal at a lower temperature than does hydrated complex **2**.

The origin of the faster rate of tunnelling for complex **3** than **2** is unclear. One possibility is that hydrated complex **2** has a $S = 10$ ground state as found for complex **1**, whereas complex **2** has a $S = 9$ ground state. The barrier height Δ in the double-well potential-energy diagram is equal to $\Delta = S^2|D|$, where D gauges the axial zero-field splitting ($D\hat{S}_{z^2}$) in the ground state. The smaller thermal barrier (Δ) for a $S = 9$ complex would also lead to larger tunnelling rates. A second possibility is that complexes **2** and **3** both have $S = 10$ ground states, but there are larger higher-order (quartic) zero-field interactions present for complex **3** and this leads to a faster tunnelling. Finally, the differences in rates between complexes **2** and **3** could be due to differences in rates of positioning a Mn_{12} complex into the $m_s = -3$ level from which tunnelling occurs.

High-field EPR experiments are in progress to determine whether complexes **2** and **3** differ in their ground-state spins. Understanding the differences in hysteresis loops between complexes **2** and **3** should give insight into the unknown mechanism of magnetization tunnelling. This is essential if the potential application of single-molecule magnets to memory devices is to be realized.

This work was supported by the National Science Foundation. The W. A. Keck Foundation provided funds for the SQUID magnetometer used in the ac susceptibility experiments.

Footnotes and References

* E-mail: dhendrickson@ucsd.edu

† *Crystal data*: $C_{128}H_{126}Mn_{12}O_{51}$ **2**: $M_w = 3139.46$, monoclinic, space group *I*2/*a*, $a = 29.2794(4)$, $b = 32.3271(4)$, $c = 29.8738(6)$ Å, $\beta = 99.2650(10)°$, $U = 27907.2(8)$ Å^3, $Z = 8$, $T = 223(2)$ K, μ(Mo-Kα) = 11.31 cm^{-1}, $D_c = 1.488$ g cm^{-3}, $R(F) = 0.0880$ for 13048 observed independent reflections ($4 \leqslant 2\theta < 56°$).

$C_{136}H_{128}H_{128}Mn_{12}O_{50}$ **3**: $M_w = 3221.66$, monoclinic, space group *C*2/*c*, $a = 40.4589(5)$, $b = 18.2288(2)$, $c = 26.5882(4)$ Å, $\beta = 125.8359(2)°$, $U = 15897.1(4)$ Å^3, $Z = 4$, $T = 193(2)$ K, μ(Mo-Kα) = 7.94 cm^{-1}, $D_c = 1.346$ g cm^{-3}, $R(F) = 0.1021$ for 7155 observed independent reflections ($4 \leqslant 2\theta < 56°$).

For complex **2** three solvate H_2O molecules were located. The 4-methylbenzoic acid solvate molecule of complex **3** is highly disordered. CCDC 182/636.

1 B. Schwarzschild, *Phys. Today*, January 1997, 17.
2 E. M. Chudnovsky, *Science*, 1996, **274**, 938.
3 S. M. J. Aubin, M. W. Wemple, D. M. Adams, H.-L. Tsai, G. Christou and D. N. Hendrickson, *J. Am. Chem. Soc.*, 1996, **118**, 7746.
4 R. Sessoli, D. Gatteschi, A. Caneschi and M. A. Novak, *Nature*, 1993, **365**, 141; D. Gatteschi, A. Caneschi, L. Pardi and R. Sessoli, *Science*, 1994, **265**, 1054.
5 R. Sessoli, H.-L. Tsai, A. R. Schake, S. Wang, J. B. Vincent, K. Folting, D. Gatteschi, G. Christou and D. N. Hendrickson, *J. Am. Chem. Soc.*, 1993, **115**, 1804.
6 J. R. Friedman, M. P. Sarachik, J. Tejada and R. Ziolo, *Phys. Rev. Lett.*, 1996, **76**, 3830.
7 L. Thomas, F. Lionti, R. Ballou, D. Gatteschi, R. Sessoli and B. Barbara, *Nature*, 1996, **383**, 145.
8 J. Tejada, R. F. Ziolo and X. X. Zhang, *Chem. Mater.*, 1996, **8**, 1784.

Received in Bloomington, IN, USA; 21st August 1997; 7/06144G